

# A Study of the Molecular Sources of Nonideal Osmotic Pressure of Bovine Serum Albumin Solutions as a Function of pH

Kalpana M. Kanal, Gary D. Fullerton,\* and Ivan L. Cameron

Department of Radiology, The University of Texas Health Science Center at San Antonio, San Antonio, Texas, USA

**ABSTRACT** The nonideal osmotic pressure of bovine serum albumin (BSA) solutions was studied extensively by Scatchard and colleagues. The extent of pH- and salt-dependent nonideality changes are large and unexplained. In 1992, Fullerton et al. derived new empirical expressions to describe solution nonideal colligative properties including osmotic pressure (Fullerton et al. 1992. *Biochem. Cell Biol.* 70:1325–1331). These expressions are based on the concepts of volume occupancy and hydration force. Nonideality is accurately described by a solute/solvent interaction parameter  $I$  and an “effective” osmotic molecular weight  $A_e$ . This paper uses the interaction-corrected nonideal expressions for osmotic pressure to calculate the hydration  $I$  values and “effective” osmotic molecular weight of BSA,  $A_e$ , as a function of pH. Both factors vary in a predictable manner due to denaturing of the BSA molecule. Both contribute to an increase in osmotic pressure for the same protein concentration as the solution pH moves away from the isoelectric point. Increased nonideality is caused by larger hydration resulting from larger solvent-accessible surface areas and by the decrease in “effective” osmotic molecular weight,  $A_e$ , due to segmental motion of denatured (filamentous) molecules.

## INTRODUCTION

Ideal colligative properties of solutions (freezing point depression, boiling point elevation, vapor pressure depression, and osmotic pressure) depend on the number of solute particles per unit volume of solvent. Real solutions deviate significantly from ideal behavior and make it necessary to use empirical equations to accurately describe solutions under high osmolality conditions. Minton showed that colligative nonideality of protein solutions results from “solute volume occupancy” acting on the thermodynamic activity of the protein (Minton, 1983). Ling corrected the ideal van’t Hoff expression for nonideal behavior of proteins by making volume or hydration mass corrections (Ling, 1984). In a recent report, Fullerton et al. (1992) proposed empirical expressions to describe solution nonideal osmotic pressure, freezing point depression, and vapor pressure based on the concepts of volume occupancy and hydration force. The new expressions described the nonideality of all three colligative properties in terms of a single dimensionless constant called the solute/solvent interaction parameter,  $I$ , and the molecular weight,  $A_s$ . The constant,  $I$ , measures the occupancy volume of the solute. More recently, it was shown that filamentous molecules require a second nonideality parameter called the “effective” osmotic molecular weight,  $A_e$ .

This paper uses the new expressions to study nonideal osmotic pressure of bovine serum albumin (BSA) as a function of pH. Its purpose is to improve understanding of the variation in osmotic pressure of protein solutions as a function of pH, and to determine the molecular sources of large

increases in osmotic pressure when proteins are denatured. Freezing point depression studies of polyethylene glycol solutions (PEG) (Zimmerman et al., 1993) showed two sources of nonideality: (a) large solute/solvent interactions,  $I$  values, for large solute molecules (molecular weight >1000) and (b) segmental motion of filamentous macromolecules. We hypothesize that both factors will change with denatured proteins and cause the measured osmotic pressure at the same protein concentration to increase. Calculations show that the amount of solvent-accessible surface area increases when BSA is denatured from monolayer coverage of 0.6 g H<sub>2</sub>O/g BSA to 2.8 g H<sub>2</sub>O/g BSA (Miller et al., 1987). The measured “effective” osmotic molecular weight,  $A_e$ , is predicted to decrease from the chemical value  $A_s = 66,336$  to approximately one quarter of that value when denatured, if we assume filamentous proteins behave similarly to other such flexible polymers.

Many proteins are denatured by moving the solution pH away from the isoelectric point. BSA has an isoelectric point at pH 5.4. Above or below this point, electrostatic repulsion from “like” charges favors the denatured state. This is especially true at low cosolute salt concentrations. Measurement of osmotic pressure as a function of pH allows us to quantitate the contributions of both segmental motion and increased solvent-accessible surface area. As shown here both factors are important, but segmental motion dominates at low BSA concentrations whereas hydration is most important at high concentrations.

## EXPERIMENTAL PROCEDURES

### Materials

BSA (molecular weight = 66,336, 98–99% albumin, heat-shock fraction) was purchased from Sigma Chemical Company (St. Louis, MO). It was stored in a refrigerator at 4°C.

Received for publication 3 August 1993 and in final form 3 August 1993.

Address reprint requests to Dr. Gary D. Fullerton, Department of Radiology, University of Texas, Health Science Center at San Antonio, 7703 Floyd Curl Drive, San Antonio, TX 78284-7800.

© 1994 by the Biophysical Society

0006-3495/0/01/153/08 \$2.00

## Methods

A 50 mM sodium chloride (NaCl) solvent solution was made with distilled, deionized water and used at pH = 6.9. Known amounts (0.30, 0.35, 0.40, 0.45, 0.50 g) of BSA were added to different glass vials. Five milliliters of the 50 mM NaCl were added to each glass vial to make solutions of approximately 6, 7, 8, 9, 10, and 11% BSA. The BSA samples were then filtered with 0.45  $\mu$ m Acrodisc filters (Gelman Sciences, Inc., Ann Arbor, MI). The samples were kept overnight in a refrigerator at 4°C. Citrate, acetate, and Tris buffers were used for making solutions of pH 3, 4, 4.6, 5, 5.4, 6, 7.3, and 8. In each case, after the solutions were made, NaCl was added to maintain a constant solution osmolality of 0.1 osm/kg. This osmolality was measured on a Osmomat 030 freezing-point depression osmometer (UIC, Joliet, IL). A small aliquot (50  $\mu$ l) of the solution was placed in a microfuge tube. The osmometer's built-in cooling system supercooled the solution to -6.87°C. A crystallization needle was injected into the solution and once the solution was supercooled, the osmolality of the solution was displayed digitally on the osmometer. The next day, the samples were degassed in a vacuum (-96 kPa) for 10 min, and the pH was recorded immediately before osmotic pressure measurements.

## Preparation of buffers

The 50 mM sodium chloride solution was used only at a pH = 6.9. Buffers were used to make up solutions of pH 3, 4, 4.6, 5, 5.4, 6, 7.3, and 8. The preparation method is given below.

### Citrate buffer

Stock solutions consisted of buffer A (0.1 M solution of citric acid, 21.01 g in 1000 ml) and buffer B (0.1 M solution of sodium citrate, 29.41 g in 1000 ml) (Lillie, 1948) (pH 3.0). Solvent was prepared using 46.5 ml of buffer A plus 3.5 ml of buffer B, diluted to a total of 100 ml with doubly distilled deionized water.

### Acetate buffer

Stock solutions consisted of buffer A (0.2 M solution of acetic acid, 11.55 ml in 1000 ml) and buffer B (0.2 M solution of sodium acetate, 16.4 g in 1000 ml) (Walpole, 1914) (pH 4.0, 4.6, 5.0, 5.4). For pH 4.0, solvent was prepared using 41.0 ml of buffer A plus 9.0 ml of buffer B; for pH 4.6, solvent was prepared using 25.5 ml of buffer A plus 24.5 ml of buffer B; for pH 5.0, solvent was prepared using 14.8 ml of buffer A plus 35.2 ml of buffer B; and for pH 5.4, solvent was prepared using 8.8 ml of buffer A plus 41.2 ml of buffer B. All the solvents were diluted to a total of 100 ml with doubly distilled deionized water.

### Tris-maleate buffer

A buffer-grade Tris can be obtained from the Sigma Chemical Co. or from Matheson Coleman and Bell (East Rutherford, NJ) (Gomori, 1948) (pH 6.0, 7.3, 8.0). Stock solutions consisted of buffer A (0.2 M solution of Tris-maleate (24.2 g of Tris-maleate + 23.2 g of maleic acid or 19.6 g of maleic anhydride in 1000 ml)) and buffer B (0.2 M sodium hydroxide). For pH = 6.0, solvent was prepared using 50 ml of buffer A plus 26.0 ml of buffer B; for pH = 7.3, solvent was prepared using 50 ml of buffer A plus 52.5 ml of buffer B; and for pH = 8.0, solvent was prepared using 50 ml of buffer A plus 69.0 ml of buffer B. All the solvents were diluted to a total of 200 ml with double deionized water.

## Osmotic pressure measurements

An Osmomat 050 automatic, colloid osmometer (UIC Inc.) was used to make the osmotic pressure measurements. A two-layer membrane filter with a 20,000 molecular weight cut-off was used. For each pH, the chamber was rinsed with solvent overnight in the osmometer to condition the membrane.

To measure the osmotic pressure, a sample (250  $\mu$ l) was injected into the osmometer with a Hamilton syringe. Four injections were made for each concentration starting at 6% BSA, and increasing to 11% BSA. The osmotic pressure was digitally displayed once the sample reached equilibrium. The osmotic pressure for salt solutions (cm solvent) was converted to cm water by multiplying by the ratio of densities obtained from the *CRC Handbook of Chemistry and Physics* (Weast, 1981).

To determine the final BSA concentrations, an aliquot (~3 g) of each BSA solution was dried in an oven at 61°C for 3–4 days. The aliquots were then transferred to a vacuum oven at 100°C and dried for an additional day. The dried mass  $M_d$  and the mass of the solution (before dry down),  $M_{sol}$ , were measured. The solvent mass,  $M_{sv}$ , and the solute mass,  $M_s$ , were calculated gravimetrically as described previously (Fullerton et al., 1993).  $M_{sv}/M_s$  was then plotted against inverse osmotic pressure  $1/\pi$ . Linear regression analysis gave a best fit equation for each solvent pH. The y-intercept directly gives the solute/solvent interaction parameter value or  $I$  value, and the  $A_e$  is determined from the slope of the line using the equation (Fullerton et al., 1992)

$$A_e = [84.8 \times (297.15) \times D \times 1000]/S, \quad (1)$$

where 84.8 = universal gas constant (liter cm H<sub>2</sub>O °K<sup>-1</sup>/mol), 297.15 = absolute temperature °K, 1000 = conversion factor from kg to g water,  $D$  is the density correction factor ranging from 0.9989 to 1.001, and  $S$  is the slope of the line.

To determine overall experimental precision, each experiment was repeated three times for each pH level. No significant difference was observed in the results from the three experiments. The  $I$  value was calculated by obtaining the best linear regression fit to the data acquired from all three experiments at each pH. The  $A_e$  was calculated using the average of the three experiments, and the standard deviation was used to give estimates of precision for  $I$ ,  $S$ , and  $A_e$ .

## RESULTS

### Osmotic pressure versus pH

To display the trend of the measured osmotic pressure as a function of pH, we plotted measured osmotic pressure versus the pH for different concentrations of BSA (Fig. 1). Our plot showed that as the pH is decreased from 8 to 4.6, the measured osmotic pressure decreased. As the pH was decreased below 4.0, there was a sharp increase in the osmotic pressure. For pH 3.0, we could not obtain data for 10 and 11% BSA concentrations because they were out of range of the osmometer (>100 cm water) at these higher BSA concentrations. Osmotic pressure variations as great as a factor of five were observed for the same protein concentration.

The same data were next analyzed using the interaction-corrected method to give the best fit regression parameters shown in Table 1 for  $M_w/M_s$  as a function of  $1/\pi$  at each pH as shown by the dotted line for pH 6.9 in Fig. 1. The table gives the best fit to the data obtained from three experiments at each pH for all the regression parameters. These analyses gave the fitting parameters  $A_e$  and  $I$  shown in Table 2 using the methods described previously (Fullerton et al., 1992).

### Effective osmotic molecular weight $A_e$

A plot of  $A_e$  versus pH is shown in Fig. 2.  $A_e$  increased to a maximum of 79,000 at pH = 4.6 and then decreased to much lower values at higher and lower pH levels. Comparison of  $A_e$  with the chemical molecular weight,  $A_s$  = 66,336

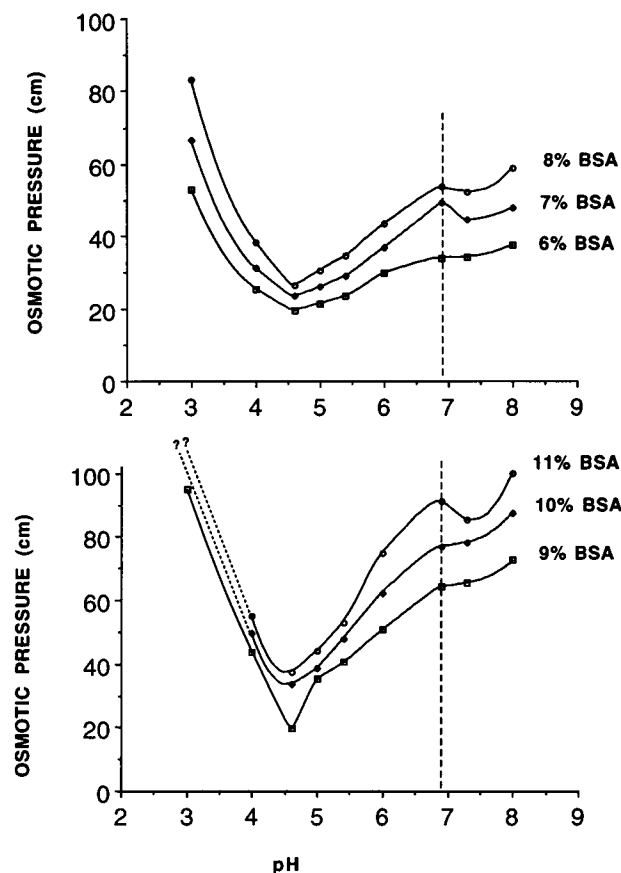


FIGURE 1 The variation in osmotic pressure as a function of pH is examined. As the pH decreases from 8 to 4.6, the osmotic pressure decreases. As the pH is decreased further, there is a steep increase in the osmotic pressure. For pH = 3, we could not obtain data for the 10% and 11% BSA concentrations since they were greater than 100 cm H<sub>2</sub>O (dashed lines), the limit of the colloid osmometer.

allows division into three regions; region A,  $A_e < A_s$  for pH < 4.0; region B,  $A_e > A_s$  for 4.0 < pH < 6.0; region C,  $A_e \approx A_s$  for pH  $\geq$  6.0.

### $I$ value

The  $I$  value is also plotted as a function of pH in Fig. 2. The  $I$  value ranges from 8.7 at pH 3.0, to a minimum of 1.4 at pH 4.6, and then increases to an intermediate value ranging between 4 and 5 at higher pH. Our results at pH 6.9 agree with those found in the literature (Zimmerman et al., 1992). This group reported an  $I$  value of  $4.34 \pm 0.08$  for a 50 mM NaCl solution.

## DISCUSSION

### Osmotic pressure versus pH

Osmotic pressure varies significantly with pH. As shown in Fig. 1, the variation of osmotic pressure as a function of pH is qualitatively similar to the observations of Scatchard et al. (1946a, b). The range of observed osmotic pressure for a single BSA concentration, however, is much greater due to

TABLE 1 Regression parameters for  $M_w/M_s$  as a function of  $1/\pi$

pH	$n$	$R^2$	Slope $\pm$ SD	Constant $\pm$ SD
3.0	12	0.98298	$643 \pm 26.8$	$8.66 \pm 0.30$
4.0	18	0.99009	$366 \pm 9.2$	$3.87 \pm 0.28$
4.6	18	0.99675	$316 \pm 4.5$	$1.41 \pm 0.16$
5.0	18	0.99852	$323 \pm 3.1$	$2.39 \pm 0.11$
5.4	18	0.99662	$331 \pm 4.8$	$3.75 \pm 0.17$
6.0	18	0.99739	$382 \pm 4.9$	$4.07 \pm 0.14$
6.9	18	0.98887	$421 \pm 11.2$	$4.61 \pm 0.30$
7.3	18	0.99293	$410 \pm 8.6$	$4.40 \pm 0.23$
8.0	18	0.96663	$410 \pm 19.0$	$5.00 \pm 0.47$

The regression parameters for  $M_w/M_s$  as a function of  $1/\pi$  are shown here. Three experiments were performed at each pH to determine any variability in experimental procedure or material preparation and technique. Because there was no significant variability observed among the three experiments, the best linear fit to the data from the three experiments was calculated. The standard deviation of the slope and the constant are also shown.  $n$  = the number of points = (number of experiments)  $\times$  (number of points per experiment) =  $3 \times 6 = 18$ . For pH = 3,  $n = 3 \times 4 = 12$ , because no data were obtained for 10% and 11% BSA concentration.

TABLE 2 Changes in "Effective" Osmotic Molecular Weight  $A_e$  and  $I$  value and as a function of pH

pH	Mean $A_e$ $\pm$ SD	Mean $I$ value $\pm$ SD
3.0	$38,300 \pm 4,623$	$8.66 \pm 0.30$
4.0	$68,800 \pm 1,976$	$3.87 \pm 0.28$
4.6	$79,300 \pm 1,382$	$1.41 \pm 0.16$
5.0	$78,200 \pm 653$	$2.39 \pm 0.11$
5.4	$76,300 \pm 1,655$	$3.75 \pm 0.17$
6.0	$66,000 \pm 1,155$	$4.07 \pm 0.14$
6.9	$60,000 \pm 1,418$	$4.61 \pm 0.30$
7.3	$61,800 \pm 1,875$	$4.40 \pm 0.23$
8.0	$60,500 \pm 4,763$	$5.00 \pm 0.47$

Changes in the  $I$  value and "effective" osmotic molecular weight,  $A_e$ , as a function of pH, are shown here. As pH increases from 3 to 8, the  $I$  value first decreases and then increases. In general, the values are near 4 for higher pH. The effective molecular weight,  $A_e$ , increases at first and then decreases as the pH increases. The values at higher pH are close to the chemical molecular weight of BSA, 66,336.

lower cosolute concentrations. A part of the BSA data from Scatchard's paper was also analyzed by Cameron et al. (1990). They have explained the decrease in osmotic pressure as the pH decreased from 8.15 to 4.19 by proposing that the amount of osmotically unresponsive solvent associated with a gram of BSA decreases as a function of pH over the range 8.15–4.19. They also questioned the variation of osmotic pressure at pH < 4.19 because no data were obtained below that pH. As our results have indicated, the osmotic pressure increases sharply below pH 4.0.

Adair's results (Adair, 1928) on hemoglobin showed that for 0.066 M KH<sub>2</sub>PO<sub>4</sub> plus 0.066 M Na<sub>2</sub>HPO<sub>4</sub> salt mixtures, in which concentration of diffusible salts is so much larger than the equivalent concentration of protein, the observed osmotic pressure of the protein is practically constant ( $\sim 10\%$ ) over the pH range 5 to 9. However, for solutions equilibrated with very dilute solutions of ammonia or carbonic acid, a greater variation (factor of 200%) in observed osmotic pressure was seen.

Zimmerman et al. (1992) showed that the change in BSA osmotic pressure at pH 6.9 increases at lower cosolute salt concentrations.

### Isoelectric point of proteins

Our data indicated minimum osmotic pressure at pH 4.6 instead of at the isoelectric point of BSA, pH 5.4, as we had anticipated. This minimum could have been caused by several factors: impure BSA, buffers causing minimum osmotic pressure to shift, and nonideal behavior of BSA. However, this observation agrees with results from the literature. Scatchard et al. (1946a,b) reported minimum osmotic pressure at pH 4.55 for BSA and attributed this location of the minimum to the nonideal behavior of the protein.

Burk and Greenberg (1930) have reported changes in osmotic pressure with pH for casein, hemoglobin, and edestin in urea solutions. In the case of casein in a 6.66 M urea solution, the minimum osmotic pressure was obtained in the pH range 4.78–4.92 which differs from the isoelectric point in aqueous solution (4.62). As the pH was decreased further, there was a sharp increase in osmotic pressure. Due to the difference in solvent properties, it was assumed that the isoelectric point of casein in urea solution would be appreciably different from that in aqueous solution.

The horse hemoglobin data (Burk and Greenberg, 1930) were obtained using phosphate buffers. Hemoglobin dissolved in 6.66 M urea solution was adjusted to various pH values with phosphate buffers. The osmotic pressure decreased with an increase in pH reaching a broad minimum from pH 7.3 to 9.0. The isoelectric point of hemoglobin was 6.7. The difference in minimum osmotic pressure was considered to be due to the different solvent properties of urea and water.

Edestin solutions were prepared by dissolving edestin in 6.66 M urea, and phosphate buffers were used to obtain the different pH values. The minimum osmotic pressure occurred over the pH range 5.7–8.9. Below pH 5.7, the osmotic pressure was found to increase sharply. This increase in osmotic pressure was attributed to Donnan membrane equilibrium. The results of Adair (1928) on hemoglobin, however, dispute their interpretation because direct measurement of the electric potential shows that only a small fraction of the variance is due to the Donnan electric potential.

From the results discussed above, it is clear that the minimum osmotic pressure occurs at a point slightly shifted from the isoelectric point. As the pH deviates significantly from this value, however, the osmotic pressure increases sharply. Both trends are observed in our results. We conclude that the changes seen in osmotic pressure with pH are due to the electrostatic repulsive forces acting between the charges on the BSA molecule. As the pH is moved from the isoelectric point, net positive or negative charges on the surface of the protein increase giving rise to electrostatic repulsion. This repulsion causes the protein to change conformation and denature resulting in higher osmotic pressure. The small deviations from the isoelectric point are probably due to less

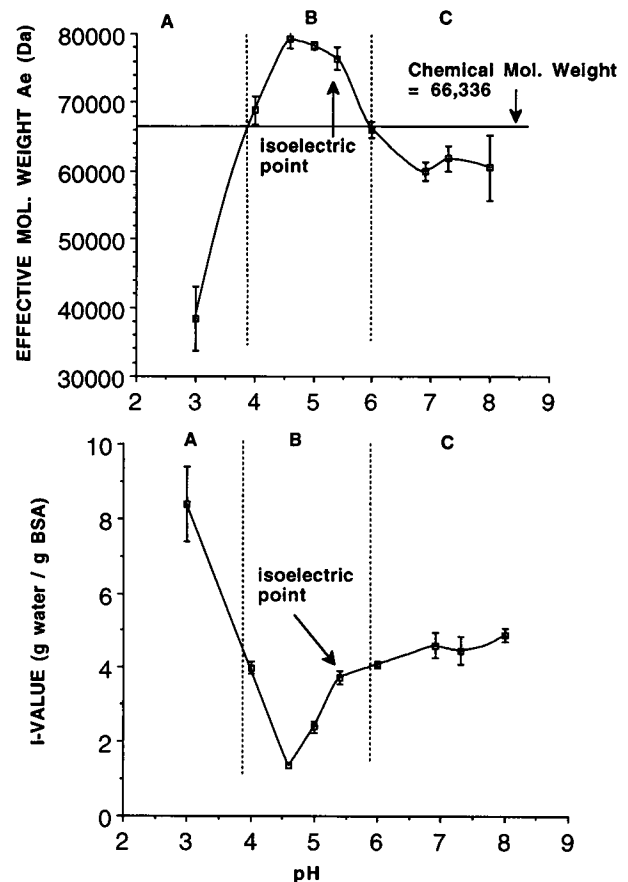


FIGURE 2 The "effective" osmotic molecular weight  $A_e$  and  $I$  value plots as a function of pH. "Effective" osmotic molecular weight  $A_e$  (upper): The horizontal line shows the true chemical molecular weight of BSA, 66,336. The vertical lines divide the graph into regions A, B, and C at the points where the horizontal line intersects the plot. The vertical bars give the standard deviation of each point. In region A, at pH = 3.0, as the protein denatures, its length increases, making the motion of its parts independent of each other. The arrows indicate motion of the segments of the denatured protein. This phenomenon is described as "segmental motion." As a result, the "effective osmotic" number of molecules in the solution does not reflect the true molecular weight, thus giving a low value for the  $A_e$ . In region B, the  $A_e$  increases due to the self-association between the BSA molecules resulting in the formation of aggregates. The aggregates move together as one molecule and thus the "effective osmotic" number of molecules in the solution give a high value for  $A_e$ . In region C, the protein denatures due to the electrostatic repulsive forces acting between the negative charges on its surface, resulting in denaturation. These forces aren't strong enough to cause the BSA to completely denature but lead to smaller values of the  $A_e$ .  $I$  value (lower): The vertical bars show the standard deviation of each point. In region A, due to the strong electrostatic repulsion force acting between the positive charges on the surface of the protein, denaturing occurs resulting in a large  $I$  value. In region B, as the pH gets closer to the isoelectric point of BSA, the charges on the surface of the protein aren't substantial enough to cause a strong repulsive force between the BSA molecules, resulting in the compactness of the protein structure leading to a lower  $I$  value. In region C, the negative charges on the surface of protein molecules repel each other leading to denaturation of the protein. However, these forces are not sufficient to cause the BSA to completely denature, thus resulting in nearly constant  $I$  values.

important solvation effects which become significant under low net charge conditions.

### Effective osmotic molecular weight, $A_e$ , versus true molecular weight, $A_s$

Previous studies of  $\beta$ -lactoglobulin, hemoglobin, BSA, and ovalbumin (Fullerton et al., 1993) showed values of  $A_e \equiv A_s$  (with root mean square error of 1.87%) when cosolute salt concentrations are high. It was recently confirmed that  $A_e < A_s$  for long filamentous molecules possessing internal molecular entropy due to segmental motion (Zimmerman et al., 1993). Zimmerman et al. (1992) quoted a value of  $58,400 \pm 1344$  for BSA in a 50 mM NaCl solution at pH 6.9. Present studies purposely used low cosolute salt concentrations ( $\sim 0.1$  osm/kg measured by freezing point depression) to promote incremental protein denaturing. Reduced salt concentration leads to increased lability which in turn corresponds to increased osmotic change. The  $A_e$  obtained is not equal to  $A_s$ .

The variation in  $A_e$  as a function of pH is shown in Fig. 2. The horizontal line shows the true chemical molecular weight of BSA,  $A_s = 66,336$ . Fig. 2 allows definition of three regions on the basis of protein surface charge: region A, where the net surface charge on the protein is positive and it is denatured; region B, where the net surface charge is close to zero and the protein is in a native state but forming aggregates; and region C, where the net surface charge is negative but the protein exists in a denatured, intermediate state. We propose that in this intermediate state, the protein is partially denatured unlike in region A where it is almost completely denatured.

### Solute/solvent interactions

Previous studies of  $\beta$ -lactoglobulin, hemoglobin, BSA, and ovalbumin (Fullerton et al., 1993) have typically yielded  $I$  values in the range 1.0 to 4.3 when proteins are in the native conformation. One negative value was also observed for ovalbumin when it is dissolved in sodium acetate. Zimmerman et al. (1992) have reported the BSA  $I$  value to be constant above 100 mM NaCl indicating that the  $I$  value is independent of the salt concentration above a minimum cosolute osmolality.

Proteins are most compact and stable near their isoelectric points (Creighton, 1984; Lehninger, 1975). This stability can be disrupted (protein unfolding) with changes in the surrounding environment. Some of these changes include a rise in the temperature, addition of denaturants, and variation of pH. The folded state of the protein has ionizable groups buried in the nonionized form that ionize only after unfolding. This unfolding can be caused by extreme changes in the pH.

Fig. 2 shows the variation in the  $I$  value as a function of pH. The direction of change of the  $I$  value is opposite to that of the effective osmotic molecular weight  $A_e$ , but both contribute increased osmotic pressure at pH extremes. The graph is divided into three regions described earlier. The average

$I$  value in region C is 4.5 which agrees closely with the value 4.34 obtained by Zimmerman et al. (1992).

### Region B, net neutral charge or isoelectric region

In this region which includes the isoelectric point of BSA, pH 5.4, the  $I$  value is very small, suggesting that the BSA is very compactly folded or in the native state. The surface of the BSA molecule at the isoelectric point is covered with charges, but the net charge is zero (Creighton, 1984; Lehninger, 1975). We hypothesize that the charges on the surface of the protein are not substantial enough to cause a strong repulsive force between the molecules, thus resulting in the compactness of the protein structure. However, because the intermolecular repulsive forces are weak, there is greater probability that the BSA molecules self-associate, resulting in the formation of aggregates. The aggregates move together as one molecule, and thus the  $A_e$  of the BSA is high, reaching a maximum value of 79,000 at a pH 4.6. This is equivalent to 20% dimerization assuming only dimer and monomer forms. Aggregation near the isoelectric point is a well known phenomenon due to reduced intermolecular electrostatic repulsion and is frequently used for protein separation by precipitation.

The lower  $I$  values as shown in Fig. 2 agree with their interpretation; an overlap of inherent hydration spheres associated with each BSA molecule would decrease the overall hydration value. However the 20% dimerization observed can not possibly account for all the decrease in the  $I$  value. Thus we must assume that monomers also contribute to the decrease in the solvent-accessible surface area near the isoelectric point. This is possible with retraction of previously charged and extended side chains. A second possibility could be the hydration influence due to loss of interaction between cosolute salt ions and charges on the protein. These questions cannot be fully resolved from the present experiments.

### Region A, net positive charge, denatured

In region A, it was anticipated that the  $I$  values would increase to approach those observed for filamentous molecules such as dextran and PEG (Cantu et al., submitted for publication; Zimmerman et al., 1993) when the protein was denatured. The acidic solution at pH < 5.4 results in an increase in the positive charges on the surface of the BSA molecules. This causes strong electrostatic repulsive forces forcing components to move away from one another so that "unfolding" or "denaturing" of the BSA molecule occurs (Creighton, 1984; Lehninger, 1975). Molecules also repulse one another so that little aggregation is observed. As the protein unfolds, the occupancy volume of the protein increases resulting in an increase in the  $I$  value. As a result, we get a large  $I$  value at pH 3.

BSA and other proteins are frequently denatured by moving their pH far from the isoelectric point. Due to the low salt concentration, the proteins are highly unstable, and thus in this region we get a small  $A_e$  (39,000). The effective osmotic

molecular weight,  $A_e$ , is significantly less than the molecular weight  $A_s$ . It is well known that denaturing increases as  $|\text{pH}-5.4|$  increases due to intramolecular electrostatic repulsion (Creighton, 1984; Lehninger, 1975). As the protein denatures, its length increases making the motion of its parts independent of each other. This phenomenon was described as "segmental motion" and was reported by Haller (1929). The number of "effective osmotic" molecules in the solution do not reflect the true molecular weight. This phenomenon has been described by Minton (1983) in terms of the radius of gyration due to independent filamental motion. This decrease in  $A_e$  is not as large as reported for dextran and PEG. Two factors could ameliorate the expected decrease in  $A_e$ : (a) the protein may not be completely denatured and (b) the protein may be less flexible than PEG.

### Region C, net negative charge, partially denatured, intermediate state

In region C, the same phenomenon occurs as in region A, but instead of positive charges there is an increase in the negative charges on the surface of the protein molecules. In this case, however, smaller  $I$  values were obtained suggesting that the electrostatic repulsive forces are not strong enough to cause the protein to denature completely.

The  $I$  values were nearly constant over the pH range 6 to 8, implying little change in solvent-accessible surface area. Small change in  $A_e$  was also observed, indicating increased flexibility of the BSA molecule but less than in region A. The  $A_e$  values ranged from 60,000 to 66,000. We hypothesize that this is an intermediate state in which the BSA is denatured but not to the same extent as in region A.

Thus two sources of  $A_e$  error relative to  $A_s$  are observed for low salt concentration: (a)  $A_e < A_s$  due to denaturing (segmental motion) and (b)  $A_e > A_s$  due to aggregation. Both effects are inhibited by physiological pH and high cosolute salt concentration.

### Molecular sources of osmotic nonideality

The variation in the osmotic pressure with pH can be explained in terms of two sources of nonideality. The sources of nonideality affecting the behavior of BSA are segmental motion leading to lower values of  $A_e$  and solute/solvent interactions for large solutes. To determine the dominance of these two sources over a specific BSA concentration range, a graph describing the change in osmotic pressure as a function of BSA concentration was plotted (Fig. 3). Three plots describing regions A ( $\text{pH} < 4.0$ ), B ( $4.0 < \text{pH} < 6.0$ ), and C ( $\text{pH} \geq 6.0$ ) were considered. In all the plots, the solid straight line represented the ideal plot for the true molecular weight obtained by using the following equation (Fullerton et al., 1992):

$$\pi = [1000 RT/A_s] \times M_s/M_w, \quad (2)$$

where 1000 = conversion factor from kg to g water,  $R$  is the

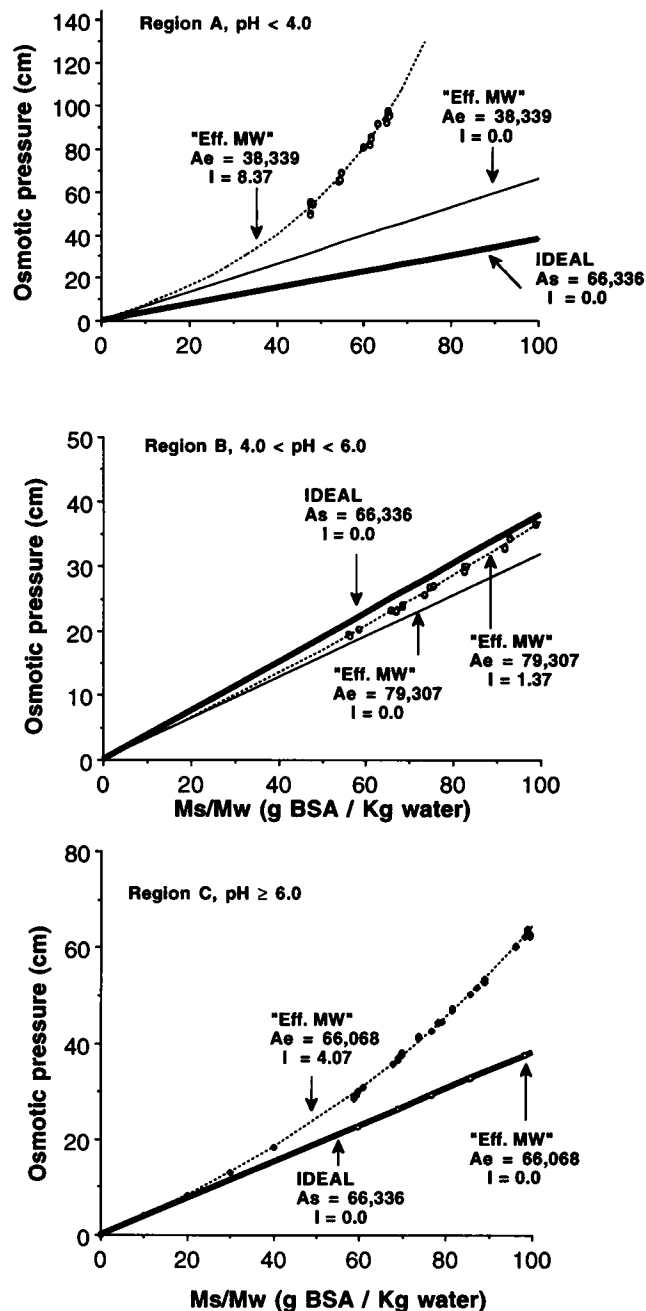
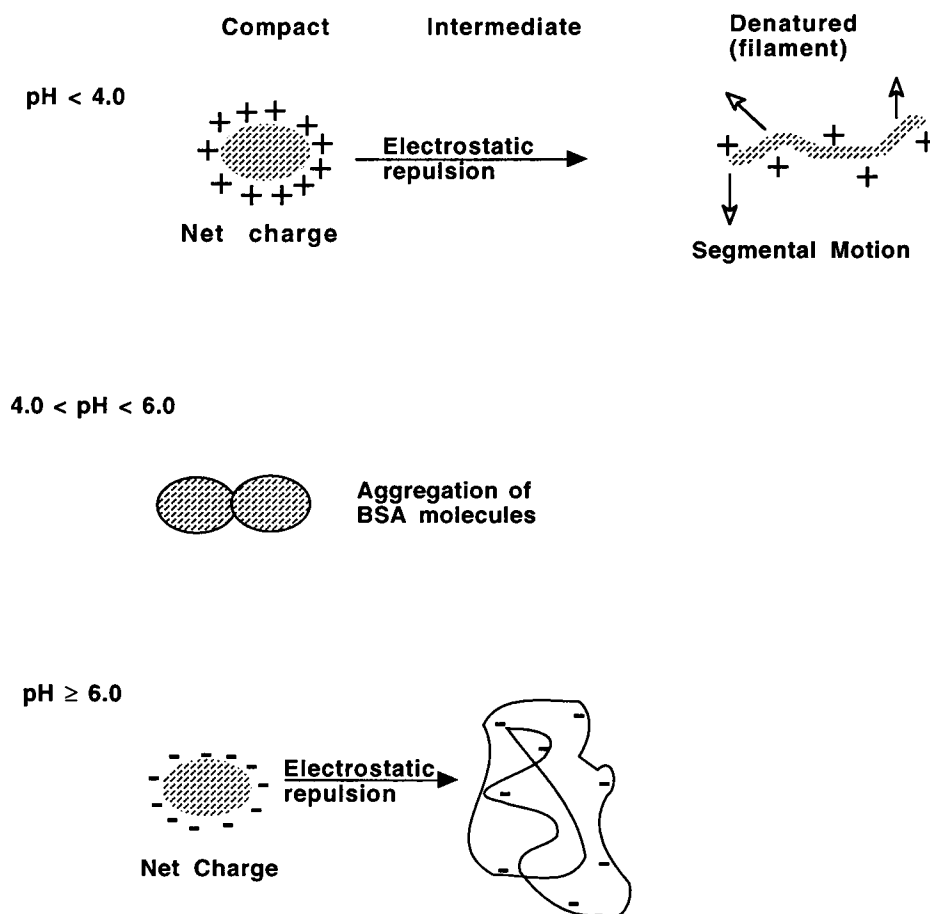


FIGURE 3 This plot shows the relative importance of the two sources of nonideality in a specific BSA concentration range. In region A, for  $\text{pH} = 3.0$ , at low concentrations, the dominant source of nonideality is segmental motion. At higher concentrations, the nonideality is mainly due to large  $I$  values resulting from the attractive/repulsive forces acting between solute and solvent molecules. In region B, for  $\text{pH} = 4.6$ , at low concentrations, the main source is aggregation leading to  $A_e$  larger than  $A_s$ . At higher BSA concentrations, opposing factors due to solute/solvent interactions and nonideality due to aggregation cancel each other out. In region C, for  $\text{pH} = 6.0$ , the effective ideal line due to segmental motion (represented by circles on the solid line) approaches the ideal line, indicating no segmental motion nonideality. The only contributing source to nonideality in this case comes from solute/solvent interactions at all the BSA concentrations.

universal gas constant (liter cm  $\text{H}_2\text{O}^\circ\text{K}^{-1}/\text{mol}$ ),  $T$  is the absolute temperature  $^\circ\text{K}$ ,  $A_s$  is the ideal molecular weight, and  $M_s/M_w$  is the mass of solute/mass of water.

**DIFFERENT CONFORMATIONS OF BSA  
AT COSOLUTE OSMOLALITY = 0.1 OSMOL/KG**



**FIGURE 4** This figure represents pictorially regions A, B, and C in Fig. 3. The charge shown on the BSA molecule is the net charge. For region A, pH < 4.0, the BSA molecule denatures giving rise to segmental motion. This direction of motion is indicated by the arrows in the figure on the extreme right. In region B, 4.0 < pH < 6.0, the BSA molecule is still compact but has formed aggregates. About 20% of the molecules are in dimer form. Finally, in region C, pH ≥ 6.0, the BSA structure changes from compact state to intermediate state. In this state, however, the BSA has not denatured to the extent causing segmental motion.

The thinner straight line described the ideal “effective” osmotic molecular weight,  $A_e$ , obtained by substituting the “effective” molecular weight in the formula above. The dashed curve or line was obtained by solving the interaction-corrected equation for  $\pi$  (Fullerton et al., 1992) so that we account for both segmental motion ( $A_e$ ) and hydration ( $I$ ):

$$\pi = S/(M_w/M_s - I), \quad (3)$$

where  $\pi$  is osmotic pressure,  $S$  is the slope of the line,  $M_w/M_s$  is the mass of water/mass of solute, and  $I$  is the solute/solvent interaction parameter value.

The values for  $S$ ,  $I$ , and  $M_w/M_s$  were taken to be the average of the three experiments performed at each pH. The circles presented the actual data obtained from the experiments.

### Region A, pH < 4.0

As shown in Fig. 3 A, the changes in osmotic pressure are due to both solute/solvent interaction and segmental motion. At low concentrations (20 g BSA/kg water), the change in osmotic pressure due to the difference between the “effective” osmotic molecular weight,  $A_e$ , line and the ideal molecular weight,  $A_s$ , line is much larger than the change due

to the dashed interaction corrected curve. This shows that at low concentrations, the nonideality due to segmental motion is the dominant factor. At higher concentrations (≥100 g BSA/kg water), however, the important nonideality source becomes solute/solvent interactions or hydration. This is read from Fig. 3 A, because the differences in osmotic pressure due to the dashed curve describing the nonideality due to “ $I$ ” are larger than the differences from the line describing nonideality due to segmental motion. Studies of native proteins (folded polymers) which are strongly cross-linked internally show little segmental motion contribution (Zimmerman et al., 1992).

### Region B, 4.0 < pH < 6.0

Fig. 3 B reveals that at low concentrations (20 g BSA/kg water), the two sources of nonideality are small. Aggregation (high  $A_e$ ) and solute/solvent interactions ( $I$  value) partially compensate for one another and cause nearly ideal response.

### Region C, pH ≥ 6.0

The ideal and the ideal effective line overlay each other in Fig. 3 C. The ideal effective line is represented by circles on

the solid line. This implies that segmental motion contributes little to nonideality at this pH. Thus, the only important contribution to nonideality comes from large solute/solvent interactions. These interactions are the primary sources of nonideal osmotic pressure at high pH.

## SUMMARY

The conclusions of this study are conceptually summarized in Fig. 4. The charges shown on the BSA molecule indicate net charge. As discussed above, for region A,  $\text{pH} < 4.0$ , the BSA molecule denatures giving rise to segmental motion (extreme right). The arrows indicate the direction of motion. In region B,  $4.0 < \text{pH} < 6.0$ , the BSA molecule is still compact but forming aggregates. We have calculated that about 20% of the molecules in this state are in dimer form. Finally, in region C,  $\text{pH} \geq 6.0$ , the BSA molecule structure changes from a compact to an intermediate state. The BSA molecule is not completely denatured in this intermediate form and thus does not show segmental motion.

Two sources of osmotic nonideality are observed: (a) large solute/solvent interaction or hydration for large solute molecules (molecular weight  $> 1000$  Da) and (b) aggregation or segmental motion of filamentous macromolecules. Both of these factors contributed to changes in osmotic pressure when the protein was denatured. The significance of either effect depends on pH region and BSA concentration. It was also concluded that the measured effective osmotic molecular weight,  $A_e$ , is not always a true indicator of the molar mass due to segmental motion and aggregation effects, which are pH dependent. This study shows greater than fivefold changes in osmotic pressure for the same protein concentration at different pH values. Changes in osmotic pressure are related to changes in protein conformation and aggregation. The largest changes are due to segmental motion of denatured filaments and increased hydration due to increased solvent-accessible surface area. This suggests that factors controlling protein conformation will likely play an important role in tissue (cellular) water content.

## REFERENCES

- Adair, G. S. 1928. A theory of partial osmotic pressures and membrane equilibria, with special reference to the application of Dalton's law to hemoglobin solutions in the presence of salts. *Proc. R. Soc. Lond. Ser. A*. 120:573–603.
- Burk, N. F., and D. M. Greenberg. 1930. The physical chemistry of the proteins in nonaqueous and mixed solvents. *J. Biol. Chem.* 87: 197–238.
- Cameron, I. L., and G. D. Fullerton. 1990. A model to explain the osmotic pressure behavior of hemoglobin and serum albumin. *Biochem. Cell Biol.* 68:894–898.
- Creighton, T. E. 1984. *Proteins: Structures and Molecular Principles*. W. H. Freeman and Co., New York.
- Fullerton, G. D., R. J. Zimmerman, C. Cantu, and I. L. Cameron. 1992. New expressions to describe solution nonideality: osmotic pressure, freezing-point depression and vapor pressure. *Biochem. Cell Biol.* 70:1325–1331.
- Fullerton, G. D., R. J. Zimmerman, K. M. Kanal, J. Floyd, and I. L. Cameron. 1993. Methods to improve the accuracy of membrane osmometry measures of protein molecular weight. *J. Biochem. Biophys. Methods*. 20: 299–307.
- Gomori, G. 1948. *Proc. Soc. Exp. Biol. Med.* 68:354.
- Haller, V. W. 1929. Zur theorie des osmotischen Druckes kolloider Losungen. *Kolloid Z.* 49:74–83.
- Lehninger, A. L. 1975. *Biochemistry*. 2nd Ed. Worth Publishers, Inc., New York.
- Lillie, R. D. 1948. *Histopathologic Technique*. Blakiston, Philadelphia.
- Ling, G. N. 1984. In *Search of the Physical Basis of Life*. Plenum Press, New York.
- Miller, S., J. Janin, A. M. Lesk, and C. Chothia. 1987. Interior and surface of monomeric proteins. *J. Mol. Biol.* 196:641–656.
- Minton, A. P. 1983. The effect of volume occupancy upon the thermodynamic activity of proteins: some biochemical consequences. *Mol. Cell. Biochem.* 55:119–140.
- Scatchard, G., A. C. Batchelder, and A. Brown. 1946a. Preparation and properties of serum and plasma proteins. VI. Osmotic equilibria in solutions of serum albumin and sodium chloride. *J. Am. Chem. Soc.* 68: 2320–2329.
- Scatchard, G., A. C. Batchelder, A. Brown, and M. Zosa. 1946b. Preparation and properties of serum and plasma proteins. VII. Osmotic equilibria in concentrated solutions of serum albumin. *J. Am. Chem. Soc.* 68: 2610–2612.
- Walpole, G. S. 1914. *J. Chem. Soc.* 105:2501.
- Weast, R. C. 1981. *CRC Handbook of Chemistry and Physics*. 62nd Ed. CRC Press, Boca Raton, FL. D232–D233.
- Zimmerman, R. J., J. Sanders, G. D. Fullerton, and I. L. Cameron. 1992. Osmotic pressure as a measure of protein folding behavior. *Biophys. J.* 61:346a. (Abstr.)
- Zimmerman, R. J., H. Chao, G. D. Fullerton, and I. L. Cameron. 1993. Solute/solvent interaction corrections account for nonideal freezing point depression. *J. Biochem. Biophys. Methods*. 26:61–70.